

# Chemokines modulate glycan binding and immunoregulatory activity of galectins

**Lucia Sanjurjo**

VU University Medical Center, Cancer Center Amsterdam

**Iris Schulkens**

VU University Medical Center, Cancer Center Amsterdam

**Pauline Touarin**

Institut de Microbiologie de la Méditerranée (IMM),

**Roy Heusschen**

VU University Medical Center, Cancer Center Amsterdam

**Ed Aanhane**

VU University Medical Center, Cancer Center Amsterdam

**Kitty Castricum**

Amsterdam UMC location VUmc, Department of Radiation Oncology, Cancer Center Amsterdam,

**Tanja de Gruijl**

Department of Medical Oncology, Cancer Center Amsterdam, Amsterdam UMC, Vrije Universiteit Amsterdam, Amsterdam

**Ulf Nilsson**

Lund University

**Hakon Lefler**

Lund University <https://orcid.org/0000-0003-4482-8945>

**Arjan Griffioen**

VU University Medical Center, Cancer Center Amsterdam

**Latifa Elantak**

Institut de Microbiologie de la Méditerranée (IMM)

**Rory Koenen**

Maastricht University

**Victor Thijssen** (✉ [v.thijssen@amsterdamumc.nl](mailto:v.thijssen@amsterdamumc.nl))

VU University Medical Center, Cancer Center Amsterdam <https://orcid.org/0000-0002-6146-1842>

---

## Article

**Keywords:** galectins, immunoregulatory activity

**Posted Date:** March 9th, 2021

**DOI:** <https://doi.org/10.21203/rs.3.rs-275662/v1>

**License:**  This work is licensed under a Creative Commons Attribution 4.0 International License.

[Read Full License](#)

---

**Version of Record:** A version of this preprint was published at Communications Biology on December 1st, 2021. See the published version at <https://doi.org/10.1038/s42003-021-02922-4>.

## **Chemokines modulate glycan binding and immunoregulatory activity of galectins.**

Lucía Sanjurjo<sup>1</sup>, Iris A. Schulkens<sup>1</sup>, Pauline Touarin<sup>2</sup>, Roy Heusschen<sup>1</sup>, Ed Aanhane<sup>1</sup>, Kitty C.M. Castricum<sup>3</sup>, Tanja D. De Gruijl<sup>1</sup>, Ulf J. Nilsson<sup>4</sup>, Hakon Leffler<sup>5</sup>, Arjan W. Griffioen<sup>1</sup>, Latifa Elantak<sup>2</sup>, Rory Koenen<sup>6</sup>, Victor L.J.L. Thijssen<sup>1,3,7</sup>

- 1) Amsterdam UMC location VUmc, Department of Medical Oncology, Cancer Center Amsterdam, Amsterdam, The Netherlands.
- 2) Laboratoire d'Ingénierie des Systèmes Macromoléculaires (LISM), Institut de Microbiologie de la Méditerranée (IMM), CNRS - Aix-Marseille Université UMR7255, Marseille, France.
- 3) Amsterdam UMC location VUmc, Department of Radiation Oncology, Cancer Center Amsterdam, Amsterdam, The Netherlands.
- 4) Lund University, Department of Chemistry, Centre for Analysis and Synthesis, Lund, Sweden
- 5) Lund University, Department of Laboratory Medicine, Section MIG, Lund, Sweden.
- 6) Maastricht University, Department of Biochemistry, Cardiovascular Research Institute Maastricht (CARIM), Maastricht, the Netherlands
- 7) Corresponding author:  
Victor L.J.L. Thijssen, PhD  
Amsterdam UMC location VUmc, Department of Radiation Oncology, Cancer Center Amsterdam, De Boelelaan 1118, 1081 HV Amsterdam, The Netherlands. phone: +31-20-4441067, fax: +31-20-4443844, mail: v.thijssen@amsterdamumc.nl

## **Disclosures:**

H.L. and U.J.N are shareholders in Galecto Biotech AB, a company developing galectin inhibitors

## **Abstract**

Galectins are versatile glycan-binding proteins involved in immunomodulation. Increasing evidence suggests that galectins can control the immunoregulatory function of cytokines and chemokines through direct binding. Here, we report a new inverse mechanism by which chemokines control the immunomodulatory function of galectins. In a galectin-chemokine interaction screen we identified several specific galectin-chemokine binding pairs, including galectin-1/CXCL4. NMR analyses showed that CXCL4 binds on the surface edge of the galectin-1  $\beta$ -sheet causing changes in the galectin-1 carbohydrate binding site. Consequently, the interaction with CXCL4 altered the glycan binding affinity and specificity of galectin-1. With regard to immunomodulation, CXCL4 potentiated the apoptotic activity of galectin-1 on activated peripheral blood mononuclear cells. The potentiation of apoptosis specifically affected CD8<sup>+</sup> T cells, while no effect was observed in CD4<sup>+</sup> T cells. An opposite regulatory activity was found for another galectin-chemokine pair, i.e., galectin-9/CCL5. While CCL5 reduced the apoptosis induction by galectin-9 in activated PBMCs, this was only statistically significant for CD4<sup>+</sup> T cells and not for CD8<sup>+</sup> T cells. Collectively, the current study describes a novel immunomodulatory mechanism in which specific galectin-chemokine interactions control the glycan-binding activity and immunoregulatory function of galectins.

## Introduction

The human glycome is a complex and dynamic collection of cellular glycans and glycoconjugates that are involved in a plethora of cellular functions. Alterations in the glycan composition have been linked to different pathologies including genetic disorders, immune diseases and cancer <sup>1</sup>. In vertebrates, the information that is encoded by the glycome is deciphered by specific glycan binding proteins, called lectins. Interestingly, the complex repertoire of the glycome greatly exceeds the number of lectins <sup>1</sup>. This suggests that specific mechanisms exist to regulate and fine-tune lectin binding affinity in order to cover the broad spectrum of the glycome.

Recently, it was shown that galectin-3, a member of the galectin protein family, can form heterodimers with the chemokine CXCL12. While galectins are known to exert their function by binding to glycoconjugates <sup>2</sup>, the interaction was found to be glycan-independent and to hamper CXCL12 activity <sup>3</sup>. Apart from galectin-3/CXCL12, the authors found interactions of other chemokines with galectin-3 or galectin-1 <sup>3</sup>. These observations support our previous finding that a chemokine-like peptide can directly bind to different members of the galectin family <sup>4,5</sup>. We described that the heterodimerization induces changes in the galectin protein structure which affects the glycan-binding affinity and specificity of galectin-1 <sup>4,5</sup>. More recently, modulation of glycan-binding activity was also observed in response to the interaction of galectin-1 with a specific fragment of the pre-B-cell receptor <sup>6,7</sup>. Collectively, these findings suggest that heterodimerization of galectins with other proteins could represent a mechanism to regulate galectin-glycan interactions. Such a mechanism would significantly extend the functionality of this glycome-decoding protein family. Whether chemokines could represent a protein family that regulates galectin function remains unexplored.

In the present study, we present evidence that the galectin-chemokine heterodimerization can indeed serve as a mechanism to modulate galectin glycan-binding and function. We found specific interactions between different chemokines and two immunomodulatory galectins i.e., galectin-1 and galectin-9. Focusing on the interaction between platelet factor 4 (PF4/CXCL4) and galectin-1, we show that the interaction modifies the glycan-binding properties of galectin-1 by inducing changes within its carbohydrate binding site. Moreover, we provide evidence that this interaction can modulate the immunomodulatory activity of galectin-1 as well as of galectin-9 on specific T cell subsets. Our

findings provide the first evidence of galectin-chemokine cross-talk which can serve as a regulatory mechanism to guide and fine-tune glycoconjugate-galectin interactions leading to specific cellular responses.

## Materials and Methods

### *Materials*

Recombinant galectin-1 and galectin-9 were in-house produced or purchased from R&D systems. For fluorescent anisotropy and apoptosis assays, the oxidation resistant mutant galectin-1, i.e., galectin-1 C3S (in-house produced) was used. Chemokines CXCL4 and CCL5 were either in-house produced<sup>8</sup> or purchased from R&D systems. All other chemokines and cytokines were purchased from R&D systems. Anginex was a kind gift from prof. K. Mayo (University of Minnesota, Minneapolis, USA). Antibodies were purchased from BD Biosciences unless indicated otherwise.

### *Primary cells and cell lines*

The human leukemia cell line Jurkat was maintained in RPMI 1640 2 mM glutamine medium (Gibco) supplemented 10% heat-inactivated fetal bovine serum (Invitrogen), 100 U/mL penicillin and 100 µg/mL streptomycin (Invitrogen). Cells were cultured in a humidified incubator at 37°C and 5% CO<sub>2</sub>. Peripheral blood mononuclear cells (PBMCs) were isolated from buffy coats from healthy donors (Sanquin) by density gradient centrifugation using Lymphoprep (Nycomed Pharma). Recovered cells were washed twice in sterile PBS with 0.1% bovine serum albumin and resuspended in RPMI-1640 2 mM glutamine (Gibco), containing 10% heat-inactivated fetal bovine serum (Invitrogen), 100 U/mL penicillin and 100 µg/mL streptomycin (Invitrogen). When indicated, PBMCs were treated with 1 µg/mL phytohemagglutinin-L (PHA-L, Invitrogen) for 24 hours prior to stimulation with galectins/cytokines. All studies involving human samples were conducted following the Declaration of Helsinki principles and current legislation on the confidentiality of personal data.

### *Spot blot*

Spot blot analysis was performed with 10 µL drops containing 3 µg of the specific proteins that were spotted onto a nitrocellulose membrane. The membrane was blocked with Odyssey blocking buffer (LI-COR Biosciences) for 1 hour, washed with PBS/0.1% Tween, and incubated with 1 µg/ml recombinant galectin-1 in PBS/0.1% Tween for 1 hour. After washing with PBS/0.1% Tween, the membrane was incubated with rabbit anti-galectin-1 antibody (1:1000, Peprotech) for 1 hour.

Following three washing steps, the secondary antibody (goat anti-rabbit IRDye 800CW, 1:10000, LI-COR Biosciences) was applied for 1 hour. Finally, the membrane was washed twice with PBS/0.1% Tween and rinsed in PBS. Images were obtained by scanning the membrane with the Odyssey infrared imaging system (LI-COR Biosciences).

#### *Gel-shift analysis*

For gel-shift analysis, 2 µg of the specific proteins were combined in a total volume of 10 µL in PBS and incubated together with 2 µL DSS (Disuccinimidyl suberate, Thermo Scientific) for 2 hours on ice to fix existing protein interactions. Where indicated, 25 mg/mL heparin or 5 mM lactose (Sigma Aldrich) was added. The reaction was quenched with 1 µL Tris buffer pH 7.5 for 15 minutes at room temperature. Subsequently, the protein mixture was suspended in Laemmli sample buffer (Biorad) supplemented with 1:20 β-mercapto-ethanol, boiled for 5 minutes and subjected to SDS-PAGE followed by Western immunoblotting using anti-galectin-1 antibody (1:1000, Peprotech).

#### *SDS-PAGE gel electrophoresis and Western blotting*

The protein samples were separated by gel-electrophoresis on a 15% polyacrylamide gel and transferred onto PVDF membranes (Millipore) following standard protocols. Membranes were blocked with Odyssey blocking buffer (LI-COR Biosciences) for 1 hour and incubated overnight at 4°C with a primary antibody. The membranes were washed three times in PBS/0.1% Tween and subsequently incubated with the appropriate secondary IRDye-labeled antibody (LI-COR Biosciences) for 1 hour. Finally, the membranes were washed two times with PBS/0.1% Tween and rinsed in PBS. Images were obtained by scanning the membrane with the Odyssey infrared imaging system (LI-COR Biosciences).

#### *Surface plasmon resonance*

Binding kinetics between galectin-1 and CXCL4 were studied using the BIAcore 1000 biosensor system (BiaCore) as described previously<sup>4</sup>. In short, galectin-1 was covalently attached to CM5 Sensor Chips (BiaCore) using amine-coupling chemistry according to the manufacturer's instructions.



Next, binding measurements were performed at 25°C using HBS-EP buffer containing 10 mM HEPES, 150 mM NaCl, 3 mM EDTA and 0.005 % surfactant P20 adjusted to pH 7.4. Interactions between galectin-1 and CXCL4 were analyzed by injection of different CXCL4 concentrations (20 µL at a flow rate of 30 µL/minute). Flow cells were regenerated by injection of 20 µL regeneration buffer (10 mM glycine-HCl, pH 2.0). Association-rate ( $K_a$ ) and dissociation-rate ( $K_d$ ) constants were obtained by analysis of the sensorgrams using the Biaevaluation software, version 3.2. All measurements were performed at least in duplicate at all concentrations and the experiment was performed in duplo.

### *Fluorescence anisotropy*

Fluorescence anisotropy analysis was performed as described previously <sup>5,9</sup>. For these experiments, the oxidation-resistant mutant galectin-1, i.e., galectin-1 C3S, was used to avoid the necessity to add β-mercaptoethanol, which may disturb interacting glycoprotein ligands <sup>10,11</sup>. In brief, 40 µL reaction mixture containing different concentrations of galectin-1 C3S and 0.1 µM of fluorescein labeled saccharide probe either with or without 8 µM CXCL4 was incubated under slow rotary shaking for 5 minutes in black 96-well half-area polystyrene microplates. All dilutions were prepared in HEPES buffer with pH 7.4 and in the absence of salt to prevent precipitation of CXCL4. Fluorescence anisotropy of fluorescein-tagged saccharide probes was measured with excitation at 485 nm and emission at 520 nm using a PheraStarFS plate reader with software PHERAstar Mars version 2.10 R3 (BMG). Binding curves were generated by plotting anisotropy against increasing concentrations of galectin-1. Anisotropy was measured without galectin-1 ( $A_0$  representing free probe), at experimental conditions ( $A$ ) and at saturating concentrations of galectin-1 ( $A_{max}$ ). The experiments were performed at least in duplicate. For the inhibition assay, increasing concentrations of the glycoprotein asialofetuin (ASF), an inhibitor of the galectin-1-probe interaction, were added to fixed low concentrations of galectin-1C3S (0.1 µM) and synthetic high-affinity tdga-probe (0.1 µM, 3'-[4-(fluorescein-5-amidomethyl)-1*H*-1,2,3-triazol-1-yl]-3'-deoxy-β-D-galactopyranosyl 3-(3,5-dimethoxybenzamido)-3-deoxy-1-thio-β-D-galactopyranoside <sup>12</sup>) in the presence or absence of 8 µM

CXCL4. Data plotting, non-linear regression analysis and curve construction was performed with Prism 9 software (Graphpad).

### *Nuclear magnetic resonance*

For NMR experiments, galectin-1 has been produced as  $^{15}\text{N}$ -labeled protein as previously described <sup>6</sup> and prepared in 20 mM  $\text{KPO}_4$  pH 5.6 buffer with 8%  $\text{D}_2\text{O}$ . All NMR spectra were acquired at 30°C on a Bruker AVANCEIII spectrometer operating at 600 MHz and equipped with cold probe. NMR data were processed with TopSpin and analyzed with Ccpnmr Analysis <sup>13</sup>. For interaction experiments with CXCL4,  $^1\text{H}$ - $^{15}\text{N}$ -HSQC spectra have been recorded on  $^{15}\text{N}$ -labeled galectin-1 (40  $\mu\text{M}$ ) in the absence and in the presence 80  $\mu\text{M}$  of CXCL4. The same experiments have been performed with  $^{15}\text{N}$ -labeled galectin-1 (350  $\mu\text{M}$ ) in the presence of CXCL4<sup>22-54</sup> (700  $\mu\text{M}$ ). The following formula was used for extracting chemical shift perturbations (CSPs), which takes into consideration the  $^1\text{H}$  and  $^{15}\text{N}$  chemical shift range of NMR signals:  $\text{CSP (ppm)} = [\Delta\delta_{\text{HN}}^2 + (\Delta\delta_{\text{N}}^2/25)]^{1/2}$  where  $\Delta\delta_{\text{HN}}$  and  $\Delta\delta_{\text{N}}$  are, respectively, the proton and nitrogen chemical shift variations of each residue.

### *NMR-Data Driven Docking*

Models of galectin-1 in complex with CXCL4 were built with the version HADDOCK2.4 of “The HADDOCK web server for data-driven biomolecular docking” <sup>14</sup>. As starting structures, we used the structures of galectin-1 (PDB ID 2KM2) and CXCL4 (PDB ID 1F9Q). The galectin-1 and CXCL4 structures were then docked within HADDOCK. Residues of galectin-1 that showed CSPs above the threshold were considered as active Ambiguous Restraints (AIR). On the CXCL4 side, the beta-sheet residues homologous to the angonex <sup>15</sup> sequence were considered as AIR. Calculations were performed with 2,000 structures during the HADDOCK rigid body energy minimization, 400 structures during the refinement, and 200 structures during the refinement in explicit water.

### *Apoptosis assays*

For analysis of apoptosis, either  $1 \times 10^5$  Jurkat cells or PBMCs per well were plated in 24-well plates and incubated for the indicated time and concentration with galectin-1 or galectin-9 alone or in combination with the indicated concentration of chemokines.

Following treatment, Jurkat cells were washed twice in ice-cold PBS and stained with (FITC)-conjugated annexin A5 (Immunotools) and propidium iodide, following the manufacturer's instructions. Cells were subsequently analyzed using a FACSCalibur instrument (BD Biosciences).

When indicated, 0.1 M lactose (Sigma-Aldrich) or 0.1 M heparin (Leo Pharma) were added to the cell culture just prior to galectin/chemokine treatment. Experiments were performed at least in triplicate.

Following PBMC treatment, PBMCs were blocked during 20 minutes with 1% BSA/PBS at 4°C, washed in ice-cold PBS and incubated during 30 minutes at 4°C with a combination of fluorescently conjugated monoclonal antibodies against CD3, CD8, CD4 and CD14 (anti CD3-APC, anti-CD8-V500, anti-CD4-PerCP Cy5.5, anti-CD14-PE). Subsequently, cells were washed twice with 0.1% BSA/PBS and stained with (FITC)-conjugated annexin A5 (Immunotools) following the manufacturer's instructions. Data acquisition was performed using a FACSCanto II instrument (BD Biosciences). Experiments were performed using PBMCs from at least six different donors. All data were analyzed using Kaluza analysis software (Beckman Coulter).

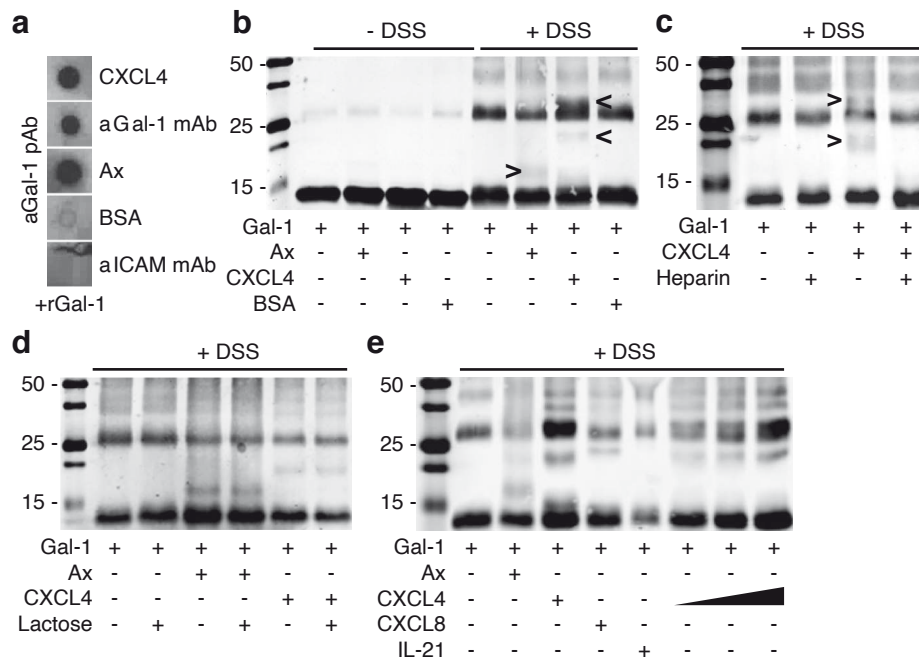
### *Statistical analyses*

Data are presented as mean  $\pm$  SD of at least three experiments unless indicated otherwise. To calculate statistically significant differences the student's t-test was used. Statistical computations were performed using Graphpad Prism software (v8 or v9) and p-values  $< 0.05$  were considered as statistically significant.

## Results

The current study aimed to explore whether galectin-chemokine interactions could serve as a mechanism to modulate galectin glycan-binding and function. First, we performed an interaction screen (**Supplementary figure 1**) and observed several specific interactions of galectin-1 and galectin-9 with different chemokines and cytokines. Based on our recent work showing complementary platelet responses induced by galectin-1 and platelet factor 4 (PF4 or CXCL4), we focused our investigation on this galectin-chemokine pair<sup>16</sup>. Spot-blot analyses showed that CXCL4 binds galectin-1 to a similar extent as the positive control peptide, i.e., anginex<sup>4</sup> (**Figure 1a**). The interaction was confirmed by gel-shift analyses where the addition of either CXCL4 ( $\pm 8$  kD) or anginex ( $\pm 4$  kD) to galectin-1 ( $\pm 14$  kD) in the presence of the crosslinking agent DSS induced a protein shift of the galectin-1 monomer corresponding to the size of each protein (**Figure 1b**). Of note, crosslinking with CXCL4 also revealed a band just above the galectin-1 dimer which could either represent a single galectin-1 monomer bound to two CXCL4 molecules or a galectin-1 dimer bound to a single CXCL4 molecule. To confirm that the interaction involved CXCL4 and was not caused by structural abnormalities due to the crosslinking agent, excess heparin was added prior to crosslinking. Heparin, a known high affinity ligand of CXCL4, served as a CXCL4 scavenger and completely neutralized the galectin-1/CXCL4 interaction (**Figure 1c**). At the same time, the addition of excess lactose, a carbohydrate ligand of galectin-1, did not prevent the interaction (**Figure 1d**). The latter confirmed that CXCL4 does not directly compete for glycan binding in the carbohydrate recognition domain of galectin-1. Furthermore, the interaction was dose-dependent and extended beyond the galectin-1/CXCL4 pair (**Figure 1e + Supplementary Figure 1**). To confirm galectin-1/CXCL4 interaction and characterize the binding kinetics of the heterodimer formation, surface plasmon resonance analysis was performed. Similar as previously described for the galectin-1:anginex interaction<sup>4</sup>, the galectin-1:CXCL4 interaction showed a 1:2 stoichiometry (single association followed by biphasic dissociation) with binding affinities in the high nanomolar and low micromolar range (**Table 1**). Collectively, these data provide clear evidence of a direct interaction between galectin-1 and CXCL4.

**Figure 1. Specific protein-protein interactions occur between galectin-1 and different chemokines**



**a)** Representative spot blot analysis. Indicated proteins were spotted onto nitrocellulose filter and following incubation with galectin-1 protein-protein interaction was revealed by staining with anti-galectin-1 antibody. Anginex (Ax) and anti-galectin-1 monoclonal antibody served as positive controls, bovine serum albumin (BSA) and anti-ICAM monoclonal antibody served as negative control.

**b)** Representative gel-shift analysis. Proteins (0.2 mg/mL) were incubated for 2 hours in the presence or absence of cross-linking agent disuccinimidyl suberate (DSS). Standard Western blot with anti-galectin-1 polyclonal antibody. The arrowheads point towards a shift of galectin-1.

**c)** Similar as in (b) but in the presence or absence of excess heparin.

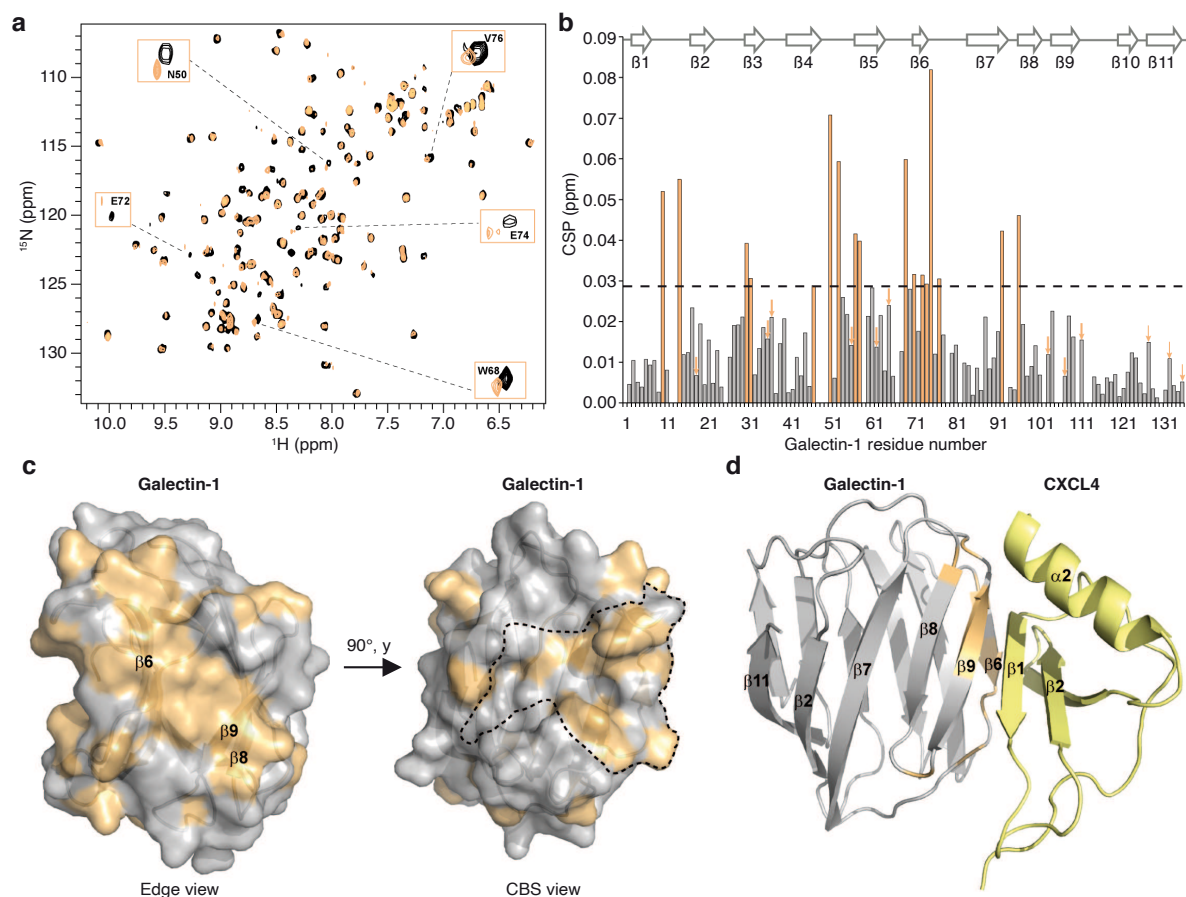
**d)** Similar as in (b) but in the presence or absence of excess  $\beta$ -lactose.

**e)** Similar as in (b) but in the presence of different cytokines or increasing concentrations of CXCL4.

To further characterize the galectin-1/CXCL4 interaction, chemical shift perturbation (CSP) mapping was performed using  $^{15}\text{N}$ -labeled galectin-1 with or without CXCL4 protein.  $^1\text{H}$ - $^{15}\text{N}$  HSQC spectra (**Figure 2a**) show that in the presence of CXCL4, several galectin-1 resonances experience CSPs (chemical shift deviations and peak intensity decrease), indicative of complex formation (**Figure 2b + Supplementary figure 2**). Remarkably, perturbed resonances localize at two different sites on galectin-1 structure: (i) a surface at the edge of the galectin-1  $\beta$ -sandwich fold (opposite to the dimer interface) (**Figure 2c**), and (ii) a surface at the carbohydrate binding site (CBS) (**Figure 2c**). The first surface is defined by perturbed resonances belonging mainly to the  $\beta 6$ ,  $\beta 8$  and  $\beta 9$  strands. Within the CBS, residues from strands  $\beta 3$  to  $\beta 6$  are perturbed upon CXCL4 interaction impacting not only the CBS core known to interact with the galactose unit but also the surrounding areas. However, our cross-linking data show that CXCL4 interaction does not compete with glycan binding activity of galectin-1, indicating that CXCL4 docks onto the perturbed surface of galectin-1 at the edge of its  $\beta$ -sheets and that this binding induces changes inside the CBS. To further investigate the structural basis of this interaction we performed NMR data-driven docking to generate a structural model of the galectin-1/CXCL4 complex. Residues from galectin-1 experiencing CSPs upon CXCL4 interaction and localized at the edge of the  $\beta$ -sandwich fold were defined as ambiguous restraints in the docking calculations. On the CXCL4 side, residues from the  $\beta$ -sheet, homologous to the anginex peptide sequence, were also considered as ambiguous restraints. In the structural model showing the best HADDOCK score, the CXCL4  $\beta$ -sheet docks onto the galectin-1 surface involving mainly  $\beta 6$  and  $\beta 9$  strands (**Figure 2d**). In addition, the CXCL4 C-terminal helix establishes contacts with strands  $\beta 8$  and  $\beta 9$  strands. To further validate the proposed structural model of the galectin-1/CXCL4 complex formation, the CXCL4  $\beta$ -sheet region (CXCL4<sup>22-54</sup>) was produced after which the interaction with  $^{15}\text{N}$ -labeled galectin-1 was tested. The perturbations observed on galectin-1 spectra corresponded to residues from the CBS and from the  $\beta 6$  and  $\beta 9$  strands (**Supplementary Figure 3**). When compared to CSPs induced by full-length CXCL4, the same regions of galectin-1 were affected with CXCL4<sup>22-54</sup> except for a few residues belonging to the  $\beta 8$  and  $\beta 9$  strands, which belong to the galectin-1 residues that interact with the CXCL4 C-terminal helix that is absent from CXCL4<sup>22-54</sup> (**Supplementary**

**Figure 3).** Therefore, these data confirm the involvement of both the CXCL4  $\beta$ -sheet and its C-terminal helix in the interaction with galectin-1.

**Figure 2. Structural characterization of the galectin-1/CXCL4 complex**



**a)** Overlay of  $^1\text{H}$ - $^{15}\text{N}$  HSQC spectra of  $^{15}\text{N}$ -labeled galectin-1 free (black trace) and bound to CXCL4 (light orange trace).

**b)** Histogram plot of CSPs observed for each galectin-1 resonance upon interaction to CXCL4. The dashed line represents  $1\sigma$  from the average CSP, thereby defining the threshold selection for the most affected residues. Light orange bars correspond to CSP above the threshold. Arrows are pointing toward residue showing significant intensity decrease upon interaction to CXCL4 (**Supplementary figure 2**). Galectin-1 secondary structures are depicted above the plot.

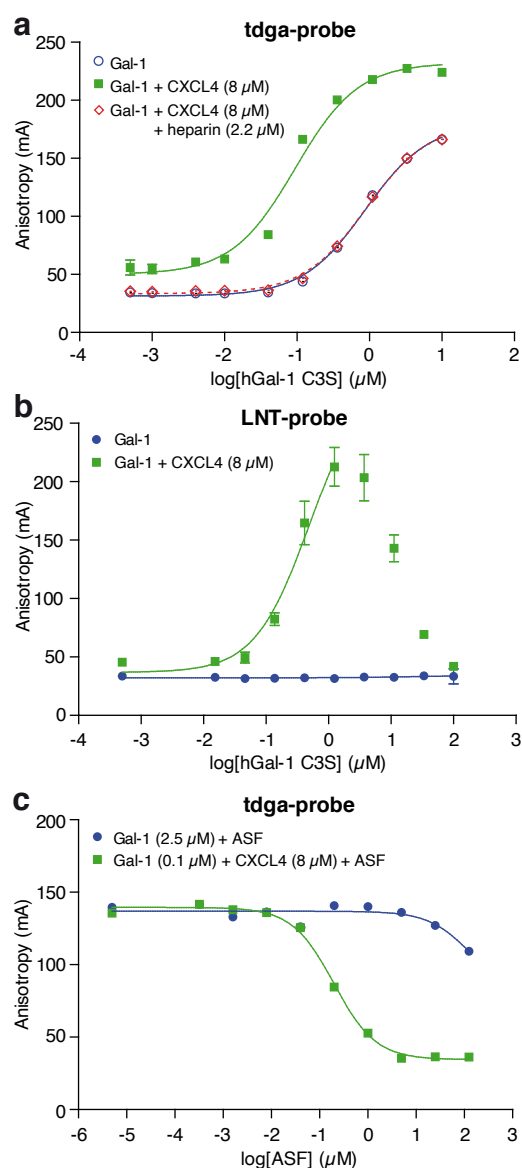
**c)** Chemical shift perturbation mapping onto galectin-1 monomer structure which is shown as a semitransparent solvent-accessible surface with a ribbon model displayed below the surface. Residues presenting CSPs above the threshold (defined in **(b)**) are colored in light orange. Main  $\beta$ -strands affected are labeled. Two galectin-1 orientations are presented: (i) the galectin-1 edge view, opposite to the dimer interface, and (ii) the CBS view with the CBS boundaries plotted in dotted lines.

**d)** The structural model of the galectin-1/CXCL4 complex. Galectin-1 is shown as grey ribbon whereas CXCL4 is colored yellow. Galectin-1 residues found at the interface of the complex and presenting CSPs above the threshold (defined in **(b)**) are colored in light orange.

Interestingly, while interacting at the edge of the galectin-1  $\beta$ -sheet, CXCL4 induced chemical shift perturbations within the galectin-1 CBS. Previously, we have shown that the direct protein-protein interactions can modulate the glycan binding affinity of galectin-1<sup>5,7</sup>. To explore whether binding of CXCL4 could also affect the carbohydrate binding affinity of galectin-1 we performed fluorescent anisotropy using a fluorescein-tagged high affinity tdga-probe<sup>12</sup>. Upon addition of CXCL4, the binding affinity of galectin-1 for this probe increased almost 10-fold to a  $K_d$  of  $0.09 \pm 0.01$  as compared to galectin-1 alone ( $K_d$  of  $0.88 \pm 0.05$   $\mu$ M) (**Figure 3a**). In line with previous results<sup>5</sup>, the  $A_{max}$  (anisotropy of the galectin-probe complex) was also increased in the presence of CXCL4, which indicates a reduced mobility of the fluorescein tag. Similar as in the gel-shift experiments, the increased binding was neutralized by the addition of heparin (**Figure 3a**). To further explore the modulation of glycan binding by CXCL4, comparable experiments were performed with a low affinity probe (lacto-N-tetraose; LNT-probe). While in the absence of CXCL4 no binding was observed due to very low  $A_{max}$ , the addition of CXCL4 induced a measurable anisotropy and binding of the LNT-probe to galectin-1 with a  $K_d$  in the range of the high-affinity tdga-probe, i.e.,  $0.48 \pm 0.18$   $\mu$ M (**Figure 3b**). Of note, at high galectin concentrations ( $>1.25$   $\mu$ M) the anisotropy levels decreased again, due to competition of the free galectin for the probe. The altered carbohydrate binding affinity was further confirmed by a competition experiment in which increasing concentrations of an unlabeled inhibitor of the galectin-1-probe interaction, i.e., the glycoprotein asialofetuin (ASF), was added to a fixed concentration of galectin-1 (the  $EC_{50}$  of the corresponding slope in the absence of ASF). In the presence of CXCL4, the inhibitory potency of ASF was more than 600-fold increased (**Figure 3c**). Altogether, these results show that heterodimerization with CXCL4 can alter the affinity and specificity of galectin-1 for glycan binding.



**Figure 3. Interactions between galectin-1 and CXCL4 affect glycan-binding affinity and specificity of galectin-1**



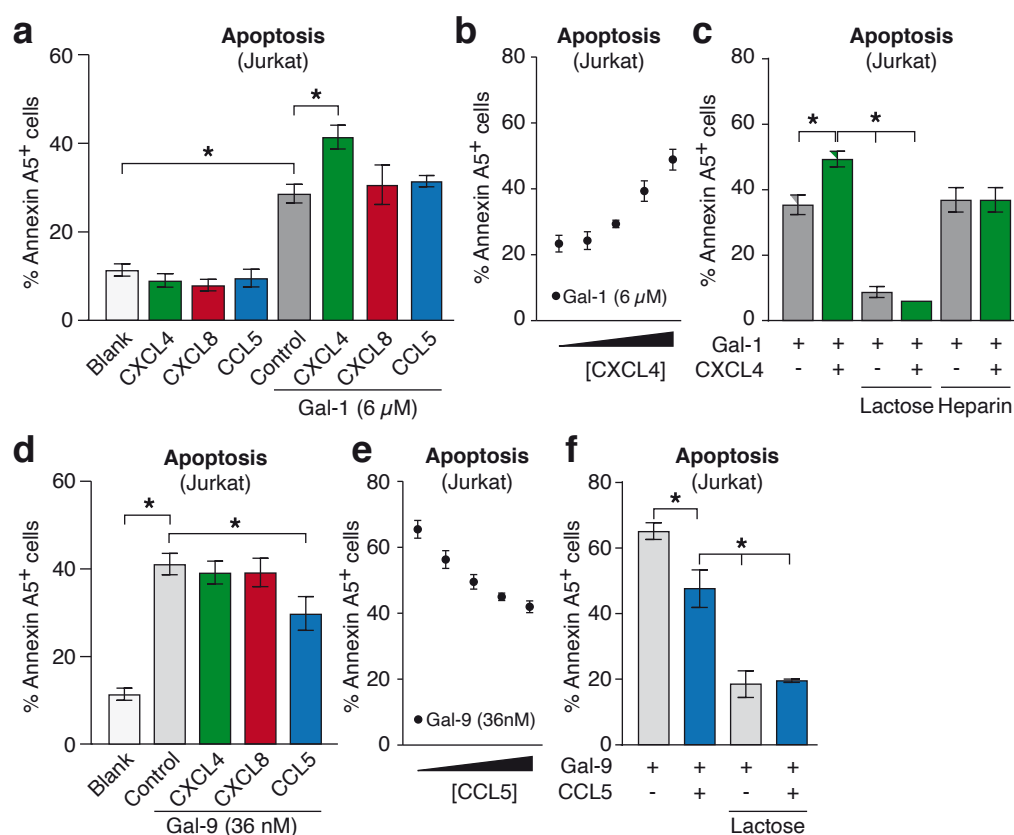
**a)** Anisotropy analyses using a fluorescently labeled high affinity thiodigalactoside amide (tdga)-probe with increasing galectin-1 concentrations in the absence (blue line, open circles) or presence (green line, closed squares) of CXCL4 and excess heparin (red line, open diamonds).

**b)** Anisotropy analyses using a fluorescently labeled low affinity lacto-N-triose (LNT)-probe with increasing galectin-1 concentrations in the absence (blue line, closed circles) or presence (green line, closed squares) of CXCL4.

**c)** Anisotropy analyses using a fluorescently labeled high affinity tdga-probe with fixed galectin-1 concentrations and increasing concentrations of an unlabeled high affinity asialofetuin (ASF)-probe in the presence (green line, closed squares) and absence (blue line, closed circles) of CXCL4.

To explore whether galectin-1/CXCL4 interactions represent an endogenous mechanism to control the function of galectin-1, we analyzed the effect of the heterodimer formation on immune cells. We focused on T cell apoptosis since galectins are known to induce apoptosis in activated T cells<sup>17-19</sup>. Indeed, in line with previous findings, we did see time- and concentration-dependent induction of T cell (Jurkat) apoptosis by galectin-1 (**Supplementary figure 4a**). Interestingly, apoptosis induction by galectin-1 was significantly increased by CXCL4 and not by CCL5 or CXCL8 (**Figure 4a**). The latter two were included since spotblot or gel shift assays indicated an interaction with galectin-1 as well (**Figure 1e** and **Supplementary figure 1**). The effects of CXCL4 were dose-dependent (**Figure 4b**) and could be blocked by the addition of either lactose, which competes for galectin-glycan binding, or heparin which scavenges CXCL4 (**Figure 4c**). CCL5 (RANTES) showed an interaction with both galectin-1 and galectin-9 (**Supplementary figure 1**), but did not affect galectin-1 function. Therefore, we explored whether CCL5 could affect galectin-9-induced T cell apoptosis. Similar as for galectin-1, treatment with galectin-9 alone resulted in a time- and concentration-dependent induction of Jurkat apoptosis (**Supplementary figure 4b**). Interestingly, the induction of apoptosis by galectin-9 was specifically inhibited by CCL5 and not by CXCL4 or IL-8 (**Figure 4d**). Again, the effect was dose-dependent (**Figure 4e**) and could be neutralized by lactose (**Figure 4f**). These results suggest that heterodimerization with specific chemokines can have opposite effects on T-cell apoptosis induction by specific galectins.

**Figure 4. Specific galectin-chemokine interactions modify the pro-apoptotic function of galectins on Jurkat cells.**



**a)** Apoptosis as determined by FACS analysis (Annexin A5<sup>+</sup> and PI<sup>+</sup> staining). Jurkat cells were incubated for 1 hour with 6 μM galectin-1 in the presence or absence of the indicated chemokines at equimolar concentrations.

**b)** Similar as in (a) but with increasing concentrations of CXCL4 (0, 1.5, 3, 6 and 12 μM).

**c)** Similar as in (a) but with the addition of either excess β-lactose or heparin

**d)** Apoptosis as determined by FACS analysis (Annexin A5<sup>+</sup> and PI<sup>+</sup> staining). Jurkat cells were incubated for 4 hours with 36 nM galectin-9 in the presence or absence of the indicated chemokines at equimolar concentrations.

**e)** Similar as in (d) but with increasing concentrations of CCL5 (0, 9, 18, 36, 72 nM).

**f)** Similar as in (d) but with the addition of excess lactose.

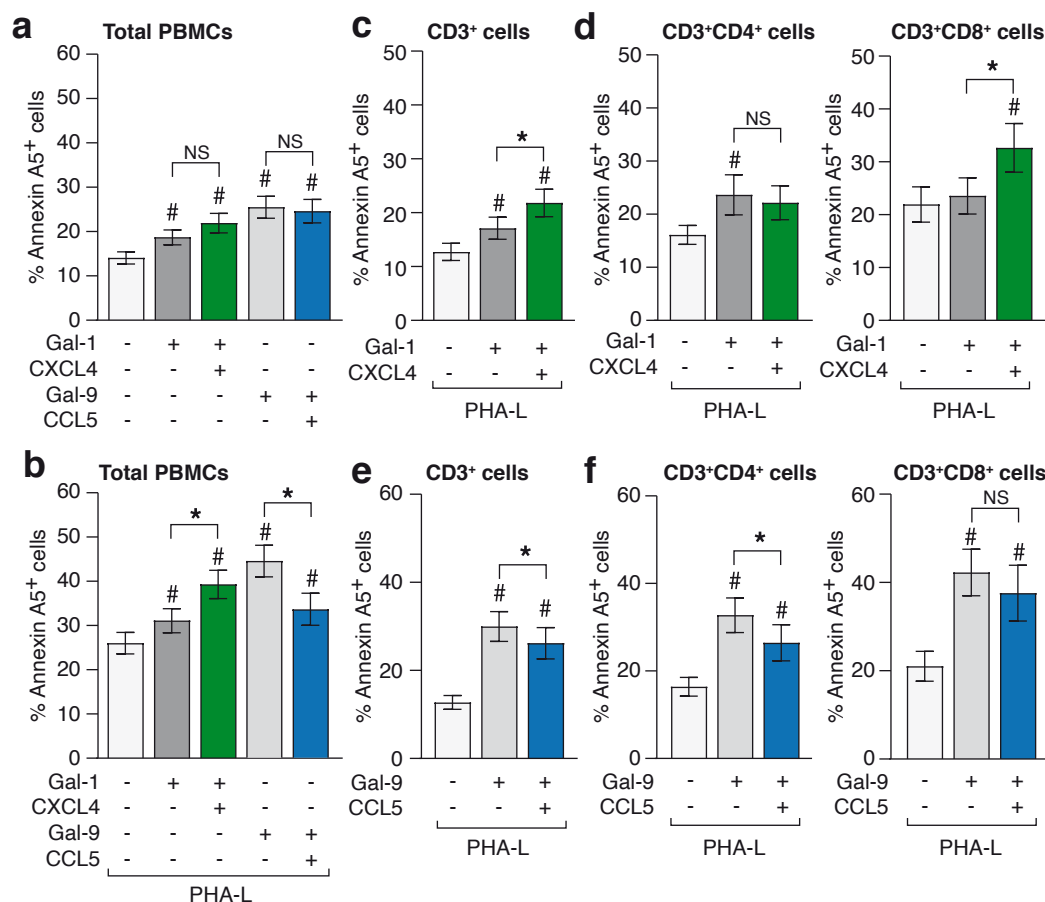
Graphs show data from at least 5 independent experiments. \*p-value <0.05

To further extend these findings, we next analyzed the effects of specific galectin-chemokine heterodimers on peripheral blood mononuclear cells (PBMCs) obtained from healthy donors. Firstly,

we evaluated the effect of galectin-chemokine heterodimers on apoptosis in resting and activated PBMCs, the latter being more susceptible to galectin-induced apoptosis<sup>19</sup>. Cell activation was induced by PHA-L lectin treatment and confirmed by CD25 surface staining (**Supplementary figure 5**). In resting PBMCs, neither CXCL4 nor CCL5 affected the induction of apoptosis by galectin-1 and galectin-9, respectively (**Figure 5a**). However, in activated PBMCs (1 µg PHA-L/mL), the pro-apoptotic effect of galectin-1 was significantly induced by CXCL4 while the pro-apoptotic effect of galectin-9 was significantly inhibited by CCL5 (**Figure 5b**). These observations corroborated our findings in Jurkat cells. Of note, in the absence of galectins, neither CXCL4 nor CCL5 induced apoptosis in resting or activated PBMCs (**Supplementary figure 6**).

To determine whether the effects could be linked to specific immune cell subsets, analyses were performed on different immune cell subpopulations, i.e. CD3<sup>+</sup> T cells, CD3<sup>+</sup>/CD8<sup>+</sup> cytotoxic T cells, CD3<sup>+</sup>/CD4<sup>+</sup> T helper cells, and CD14<sup>+</sup> monocytic cells. Regarding the galectin-1/CXCL4 heterodimer, we observed a significant increment in the percentage of apoptotic cells in CD3<sup>+</sup> cells (**Figure 5c**) upon the addition of CXCL4 to galectin-1. Within the CD3<sup>+</sup> population, the potentiation of galectin-1 apoptosis induction by CXCL4 could be mainly attributed to the CD8<sup>+</sup> cells while no effect was observed in CD4<sup>+</sup> cells (**Figure 5d**). This suggests that within the analyzed T cell subsets, CD3<sup>+</sup>/CD8<sup>+</sup> cells are particularly susceptible to galectin-1/CXCL4-induced apoptosis. The modulation of galectin-9 by CCL5 appears to display a different specificity regarding the modulation of immune cell survival. While CCL5 reduced the galectin-9-induced percentage of apoptotic CD3<sup>+</sup> cells (**Figure 5e**), this was only significant for CD3<sup>+</sup>/CD4<sup>+</sup> cells and not for CD3<sup>+</sup>/CD8<sup>+</sup> cells (**Figure 5f**). Altogether, these results suggest that galectin-chemokine heterodimers can alter the apoptotic activity of specific galectins on specific immune cell subpopulations.

**Figure 5. Specific galectin-chemokine interactions modify the pro-apoptotic function of galectins on specific immune cell subsets.**



**a)** Apoptosis as determined by FACS analysis (Annexin A5<sup>+</sup>). Peripheral blood mononuclear cells (PBMCs) were incubated for 24 hours with 12  $\mu$ M galectin-1 or 36 nM galectin-9 in the presence or absence of the indicated chemokines at equimolar concentrations.

**b)** Similar as in (a) but PBMCs were activated for 24 hours with 1  $\mu$ g/mL phytohemagglutinin-L (PHA-L) prior to treatment with galectins and chemokines.

**c-f)** Treatment similar as in (b) followed by FACS analysis with gating for specific subpopulations, i.e. CD3<sup>+</sup>, CD3<sup>+</sup>/CD4<sup>+</sup>, CD3<sup>+</sup>/CD8<sup>+</sup>. Graphs show percentage of Annexin A5<sup>+</sup> cells within the indicated populations. At least six independent experiments were performed on PBMCs from different donors. # p-value < 0.05 vs. untreated cells. \* p-value < 0.05.

## Discussion

In this study, we present evidence that specific galectins and chemokines can form heterodimers that affect the function of galectins through modifications of their glycan binding activity. In addition, we show that certain galectin-chemokine heterodimers can exert opposing immunoregulatory activity with regard to immune cell apoptosis. This reveals a previously unknown cross-talk mechanism by which galectins and chemokines can jointly control the immune response.

Both galectins and chemokines are well established (immuno)regulatory protein families that exert a plethora of biological functions, including regulation of (immune) cell recruitment, growth, differentiation, and survival <sup>20–22</sup>. Thus far, both galectins and chemokines have been considered as distinct immunomodulatory protein families. However, there is increasing evidence that suggests a link between both. For example, it has been recently shown in two studies that galectin-3 can directly interact with interferon-gamma and CXCL12, thereby affecting their activity <sup>3,23</sup>. While these findings show that galectin heterodimers can govern cytokine/chemokine function, our results show that the interaction can also regulate galectin function. This adds an entirely new level to the immunomodulatory activity of galectins. The main mechanism by which chemokines affect galectin function appears to involve modulation of the galectin glycan-binding affinity and specificity correlated to changes in the carbohydrate binding site. Previously, it has been shown that introducing mutations distal from the carbohydrate binding site can also result in small modifications in the structure of galectin-1 that affect glycan binding affinity <sup>24</sup>. In addition, carbohydrate binding in one CRD of a galectin-1 dimer has been shown to result in structural changes that influence carbohydrate affinity in the other CRD <sup>25</sup>. This is in support of a close relationship between the galectin CRD structure and ligand binding. In line with this, we have previously described that non-endogenous chemokine-like peptides can directly bind to galectins and affect glycan binding affinity <sup>5</sup>. More recently, we provided the first evidence that galectin-1 directly interacts with an endogenous protein, i.e. the pre-B cell receptor. This interaction also induces structural changes in galectin-1 which modulates glycan binding affinity, particularly with regard to LacNAc containing epitopes <sup>6,7</sup>. Our current findings extend these observations and suggest that galectin-chemokine heterodimerization represents a mechanism that allows the modification of the glycan-binding affinity and even

specificity of galectins. While the full reach of this mechanism remains to be explored, it is tempting to speculate that it represents a common mechanism in order to adapt the glycan-binding repertoire of galectins. This is supported by our current results showing heterodimer formation of different chemokines with galectin-1 and/or galectin-9 as well as by a recent study by Eckardt et al. that identified several specific chemokine interactions with galectin-1 and/or galectin-3<sup>3</sup>. Of note, while some interactions were confirmed by both Eckhardt et al. and us, e.g., gal-1/CCL5, others were not, including gal-1/CXCL4. This is most likely related to differences in experimental setup and these findings warrant further studies to unravel the specific features that govern galectin-chemokine heterodimerization and to explore the functional consequences of these heterodimeric complexes.

Regarding the functional implications, we focused here on T cell apoptosis, instigated by the established role of galectin-1 and galectin-9 in this process<sup>17-19</sup>. For example, both galectins, as well as others, can impair T cell function by inducing T cell apoptosis and skewing T cell differentiation towards a suppressive phenotype<sup>17,18,26,27</sup>. Our results confirm the previously described pro-apoptotic activity of galectin-1 and galectin-9 on T cells<sup>17,18</sup>. In addition, our current data show that this pro-apoptotic activity can be either potentiated or inhibited by specific galectin-chemokine heterodimers, i.e., gal-1/CXCL4 or gal-9/CCL5, respectively. The mechanism underlying this regulation should be further explored but it most likely involves an altered glycan-binding affinity of the specific galectin-chemokine heterodimers. For example, several T cell glycoproteins, e.g., CD3, CD7, CD43, CD45, have been linked to galectin-1-mediated T cell apoptosis<sup>19,28,29</sup>. In addition, it has been shown that the presence of specific glycan repertoires controls the ability of galectin-1 to induce apoptosis in specific T helper cells<sup>17</sup>. Thus, it can be hypothesized that (changes in) the immune cell glycan signature together with altered glycan-binding affinity of galectin-chemokine heterodimers will determine whether or not certain immune cell subset will undergo apoptosis. The observation that the effects were more potent in Jurkat cells as compared to primary PBMCs could reflect the diverse glycosylation of different immune cell subsets in the latter. Further studies should thus be aimed at deciphering which immune cell subsets are sensitive to specific galectin-chemokine heterodimers and whether this is linked to the cell surface glycan signatures.

Apart from further exploring the role of galectin-chemokine interactions in the regulation of immune cell apoptosis, our findings raise additional questions that should be addressed. For example, it is currently unknown to what extent specific galectin-chemokine heterodimerization affects other processes of the immune response, e.g., cell growth or cell differentiation/maturation. For example, it has been shown that both galectin-1 and CXCL4 are involved in Th17 differentiation<sup>30–32</sup>. Whether the galectin-1/CXCL4 heterodimers stimulate or hamper this effect is unknown. In addition, next to immune cells, both galectin-1 and CXCL4 have been shown to regulate other cell types as well, e.g., endothelial cells during angiogenesis<sup>4,33–35</sup> and platelets during hemostasis<sup>36,37</sup>. Regarding the latter, we have recently shown that galectin-1 and CXCL4 colocalize on the platelet surface<sup>16</sup>. Since co-incubation did not affect binding of galectin-1 to platelets and the observed effects on platelet function appeared to be additive rather than synergistic, it appears that this specific heterodimer does not play a major effect in platelet homeostasis. Whether this is true for other cell types and other heterodimers remains to be studied. However, given our current observations, it can be assumed that the effects of galectin-chemokine heterodimerization extend beyond the immune cell compartment.

Our finding that galectin-chemokine interactions modulate glycan binding affinity and specificity could also have implications for the efficacy of glycan-based small molecule inhibitors that target galectins<sup>38</sup> and the growing arsenal of new drugs that unleash the immune system against tumors<sup>39,40</sup>. It is essential to unravel the mechanisms by which the local tumor microenvironment (TME) controls the immune response and how these mechanisms interact<sup>17,41</sup>. Especially since tumor-controlled immunomodulation frequently involves impaired recruitment and/or function of immune cells due to the presence or absence of soluble factors like galectins and chemokines<sup>42–44</sup>. This also links to the recent findings that galectins can serve as scavenger molecules for cytokines/chemokines, thereby hampering immune cell recruitment<sup>3,23</sup>. An additional intriguing but unexplored concept is whether galectins not only scavenge but also serve as chaperones for cytokines and chemokines by directing them, in a cytokine/chemokine-specific manner, to sites displaying a specific glycosylation pattern, e.g., glycoprotein cell-surface receptors. Further insight in the reciprocal relationship between galectins and cytokines/chemokines will therefore likely benefit the development of more effective treatment strategies.



A limitation of the current study is that we only explored the effects of galectin-chemokine combinations *in vitro*. To better understand the contribution of these interactions in different biological processes, *in vivo* experiments should be performed. However, to our opinion, this first requires further insight in the complex interactions between galectins and cytokines that might occur *in vitro*. For example, it has been suggested that also heterodimers can form between different members of the galectin family<sup>45</sup> or of the chemokine family<sup>8,46</sup>. This suggests the existence of a complex regulatory network that links the local expression levels of galectins and chemokines to the complex glycome in order to regulate cellular functions *in vivo*. The present *in vitro* study adds to the understanding of this complex network and future studies should resolve to what extent the specific galectin-chemokine interactions described here contribute to *in vivo* biology.

In summary, we present evidence that galectins and chemokines can directly interact and that this heterodimerization can affect the glycan-binding properties and immunoregulatory activity of galectins. These findings suggest the existence of a reciprocal mechanism to fine-tune the activity of galectins by chemokines. A better understanding of this mechanism will provide insight in the complex process of immunomodulation and will help the development of future (immuno)therapeutic strategies.

## **Acknowledgements**

The authors thank prof. Kevin H Mayo (University of Minnesota) for providing anginex and Anita Stam for excellent technical assistance. Part of this research was supported by a grant of the Dutch Cancer Society (KWF11040 to VLT).

## References

1. Cummings, R. D. The repertoire of glycan determinants in the human glycome. *Mol Biosyst* **5**, 1087-1104 (2009).
2. Thijssen, V. L., Heusschen, R., Caers, J. & Griffioen, A. W. Galectin expression in cancer diagnosis and prognosis: A systematic review. *Biochim Biophys Acta* **1855**, 235-247 (2015).
3. Eckardt, V. et al. Chemokines and galectins form heterodimers to modulate inflammation. *EMBO Rep* e47852 (2020).
4. Thijssen, V. L. et al. Galectin-1 is essential in tumor angiogenesis and is a target for antiangiogenesis therapy. *Proc Natl Acad Sci U S A* **103**, 15975-15980 (2006).
5. Salomonsson, E., Thijssen, V. L., Griffioen, A. W., Nilsson, U. J. & Leffler, H. The anti-angiogenic peptide anginex greatly enhances galectin-1 binding affinity for glycoproteins. *J Biol Chem* **286**, 13801-13804 (2011).
6. Elantak, L. et al. Structural basis for galectin-1-dependent pre-B cell receptor (pre-BCR) activation. *J Biol Chem* **287**, 44703-44713 (2012).
7. Bonzi, J. et al. Pre-B cell receptor binding to galectin-1 modifies galectin-1/carbohydrate affinity to modulate specific galectin-1/glycan lattice interactions. *Nat Commun* **6**, 6194 (2015).
8. Koenen, R. R. et al. Disrupting functional interactions between platelet chemokines inhibits atherosclerosis in hyperlipidemic mice. *Nat Med* **15**, 97-103 (2009).
9. Sörme, P., Kahl-Knutsson, B., Huflejt, M., Nilsson, U. J. & Leffler, H. Fluorescence polarization as an analytical tool to evaluate galectin-ligand interactions. *Anal Biochem* **334**, 36-47 (2004).
10. Hirabayashi, J. & Kasai, K. Effect of amino acid substitution by sited-directed mutagenesis on the carbohydrate recognition and stability of human 14-kDa beta-galactoside-binding lectin. *J Biol Chem* **266**, 23648-23653 (1991).
11. Nishi, N. et al. Functional and structural bases of a cysteine-less mutant as a long-lasting substitute for galectin-1. *Glycobiology* **18**, 1065-1073 (2008).

12. Salomonsson, E. et al. Monovalent interactions of galectin-1. *Biochemistry* **49**, 9518-9532 (2010).
13. Vranken, W. F. et al. The CCPN data model for NMR spectroscopy: development of a software pipeline. *Proteins* **59**, 687-696 (2005).
14. van Zundert, G. C. P. et al. The HADDOCK2.2 Web Server: User-Friendly Integrative Modeling of Biomolecular Complexes. *J Mol Biol* **428**, 720-725 (2016).
15. Griffioen, A. W. et al. Anginex, a designed peptide that inhibits angiogenesis. *Biochem J* **354**, 233-242 (2001).
16. Dickhout, A. et al. Galectin-1 and platelet factor 4 (CXCL4) induce complementary platelet responses in vitro. *PLoS One* **16**, e0244736 (2021).
17. Toscano, M. A. et al. Differential glycosylation of TH1, TH2 and TH-17 effector cells selectively regulates susceptibility to cell death. *Nat Immunol* **8**, 825-834 (2007).
18. Bi, S., Earl, L. A., Jacobs, L. & Baum, L. G. Structural features of galectin-9 and galectin-1 that determine distinct T cell death pathways. *J Biol Chem* **283**, 12248-12258 (2008).
19. Perillo, N. L., Pace, K. E., Seilhamer, J. J. & Baum, L. G. Apoptosis of T cells mediated by galectin-1. *Nature* **378**, 736-739 (1995).
20. Nagarsheth, N., Wicha, M. S. & Zou, W. Chemokines in the cancer microenvironment and their relevance in cancer immunotherapy. *Nat Rev Immunol* **17**, 559-572 (2017).
21. Rabinovich, G. A. & Croci, D. O. Regulatory circuits mediated by lectin-glycan interactions in autoimmunity and cancer. *Immunity* **36**, 322-335 (2012).
22. Zlotnik, A. & Yoshie, O. The chemokine superfamily revisited. *Immunity* **36**, 705-716 (2012).
23. Gordon-Alonso, M., Hirsch, T., Wildmann, C. & van der Bruggen, P. Galectin-3 captures interferon-gamma in the tumor matrix reducing chemokine gradient production and T-cell tumor infiltration. *Nat Commun* **8**, 793 (2017).
24. López-Lucendo, M. F. et al. Growth-regulatory human galectin-1: crystallographic characterisation of the structural changes induced by single-site mutations and their impact on the thermodynamics of ligand binding. *J Mol Biol* **343**, 957-970 (2004).

25. Nesmelova, I. V. et al. Lactose binding to galectin-1 modulates structural dynamics, increases conformational entropy, and occurs with apparent negative cooperativity. *J Mol Biol* **397**, 1209-1230 (2010).
26. Stillman, B. N. et al. Galectin-3 and galectin-1 bind distinct cell surface glycoprotein receptors to induce T cell death. *J Immunol* **176**, 778-789 (2006).
27. Wada, J., Ota, K., Kumar, A., Wallner, E. I. & Kanwar, Y. S. Developmental regulation, expression, and apoptotic potential of galectin-9, a beta-galactoside binding lectin. *J Clin Invest* **99**, 2452-2461 (1997).
28. Pace, K. E., Hahn, H. P., Pang, M., Nguyen, J. T. & Baum, L. G. CD7 delivers a pro-apoptotic signal during galectin-1-induced T cell death. *J Immunol* **165**, 2331-2334 (2000).
29. Pace, K. E., Lee, C., Stewart, P. L. & Baum, L. G. Restricted receptor segregation into membrane microdomains occurs on human T cells during apoptosis induced by galectin-1. *J Immunol* **163**, 3801-3811 (1999).
30. Cedeno-Laurent, F., Opperman, M., Barthel, S. R., Kuchroo, V. K. & Dimitroff, C. J. Galectin-1 triggers an immunoregulatory signature in Th cells functionally defined by IL-10 expression. *J Immunol* **188**, 3127-3137 (2012).
31. de la Fuente, H. et al. The leukocyte activation receptor CD69 controls T cell differentiation through its interaction with galectin-1. *Mol Cell Biol* **34**, 2479-2487 (2014).
32. Affandi, A. J. et al. CXCL4 is a novel inducer of human Th17 cells and correlates with IL-17 and IL-22 in psoriatic arthritis. *Eur J Immunol* **48**, 522-531 (2018).
33. Croci, D. O. et al. Glycosylation-Dependent Lectin-Receptor Interactions Preserve Angiogenesis in Anti-VEGF Refractory Tumors. *Cell* **156**, 744-758 (2014).
34. Maione, T. E. et al. Inhibition of angiogenesis by recombinant human platelet factor-4 and related peptides. *Science* **247**, 77-79 (1990).
35. Sharpe, R. J., Byers, H. R., Scott, C. F., Bauer, S. I. & Maione, T. E. Growth inhibition of murine melanoma and human colon carcinoma by recombinant human platelet factor 4. *J Natl Cancer Inst* **82**, 848-853 (1990).

36. Pacienza, N. et al. The immunoregulatory glycan-binding protein galectin-1 triggers human platelet activation. *Faseb J* **22**, 1113-1123 (2008).
37. Eslin, D. E. et al. Transgenic mice studies demonstrate a role for platelet factor 4 in thrombosis: dissociation between anticoagulant and antithrombotic effect of heparin. *Blood* **104**, 3173-3180 (2004).
38. Hirani, N. et al. Target-inhibition of Galectin-3 by Inhaled TD139 in Patients with Idiopathic Pulmonary Fibrosis. *Eur Respir J* (2020).
39. Berraondo, P. et al. Cytokines in clinical cancer immunotherapy. *Br J Cancer* **120**, 6-15 (2019).
40. Mahoney, K. M., Rennert, P. D. & Freeman, G. J. Combination cancer immunotherapy and new immunomodulatory targets. *Nat Rev Drug Discov* **14**, 561-584 (2015).
41. Munn, D. H. & Bronte, V. Immune suppressive mechanisms in the tumor microenvironment. *Curr Opin Immunol* **39**, 1-6 (2016).
42. Sharma, P., Hu-Lieskovan, S., Wargo, J. A. & Ribas, A. Primary, Adaptive, and Acquired Resistance to Cancer Immunotherapy. *Cell* **168**, 707-723 (2017).
43. Crome, S. Q. et al. A distinct innate lymphoid cell population regulates tumor-associated T cells. *Nat Med* **23**, 368-375 (2017).
44. De Henau, O. et al. Overcoming resistance to checkpoint blockade therapy by targeting PI3K $\gamma$  in myeloid cells. *Nature* **539**, 443-447 (2016).
45. Miller, M. C. et al. Adhesion/growth-regulatory galectins tested in combination: evidence for formation of hybrids as heterodimers. *Biochem J* **475**, 1003-1018 (2018).
46. von Hundelshausen, P. et al. Heterophilic interactions of platelet factor 4 and RANTES promote monocyte arrest on endothelium. *Blood* **105**, 924-930 (2005).

**Table 1.** Rate and affinity constants for galectin-1 binding

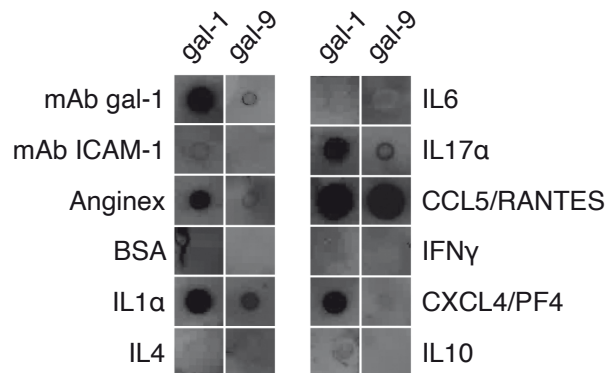
Analyte	$k_a$ (Ms <sup>-1</sup> )	$k_{d1}$ (s <sup>-1</sup> )	$k_{d2}$ (s <sup>-1</sup> )	$K_1$	$K_2$
Anginex	$6.5 \times 10^3$ ( $\pm 1.7$ )	$4.2 \times 10^{-2}$ ( $\pm 0.4$ )	$5.9 \times 10^{-4}$ ( $\pm 1.9$ )	$6.4 \pm 1.7$ $\mu$ M	$90.0 \pm 6.7$ nM
CXCL4	$1.02 \times 10^4$ ( $\pm 0.05$ )	$9.2 \times 10^{-2}$ ( $\pm 1.2$ )	$5.0 \times 10^{-3}$ ( $\pm 0.5$ )	$9.0 \pm 0.8$ $\mu$ M	$483 \pm 28$ nM
BSA	-	-	-	-	-

The association rate constant ( $k_a$ ) was obtained by plotting the  $k_{obs}$  as a function of analyte

concentration.  $K_1$  is defined as  $k_{d1}/k_a$  and  $K_2$  is defined as  $k_{d2}/k_a$ . BSA = bovine serum albumin. - = No interaction detected.

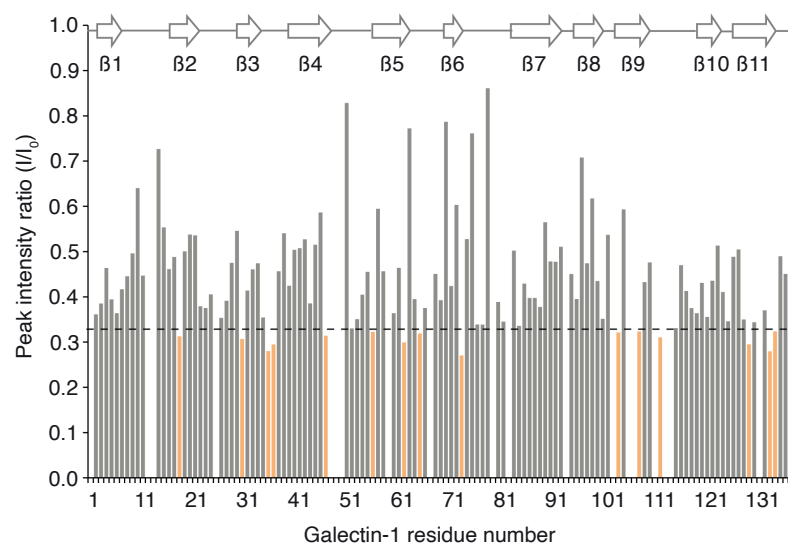
## Supplementary Figures

**Supplementary figure 1. Specific protein-protein interactions occur between galectin-1 and different cytokines/chemokines**



a) Spot blot analysis. Indicated proteins were spotted onto nitrocellulose filter and following incubation with galectin-1 or galectin-9, protein-protein interactions were revealed by staining with anti-galectin-1 antibody or anti-galectin-9 antibody. Bovine serum albumin (BSA) and anti-ICAM monoclonal antibody served as negative control.

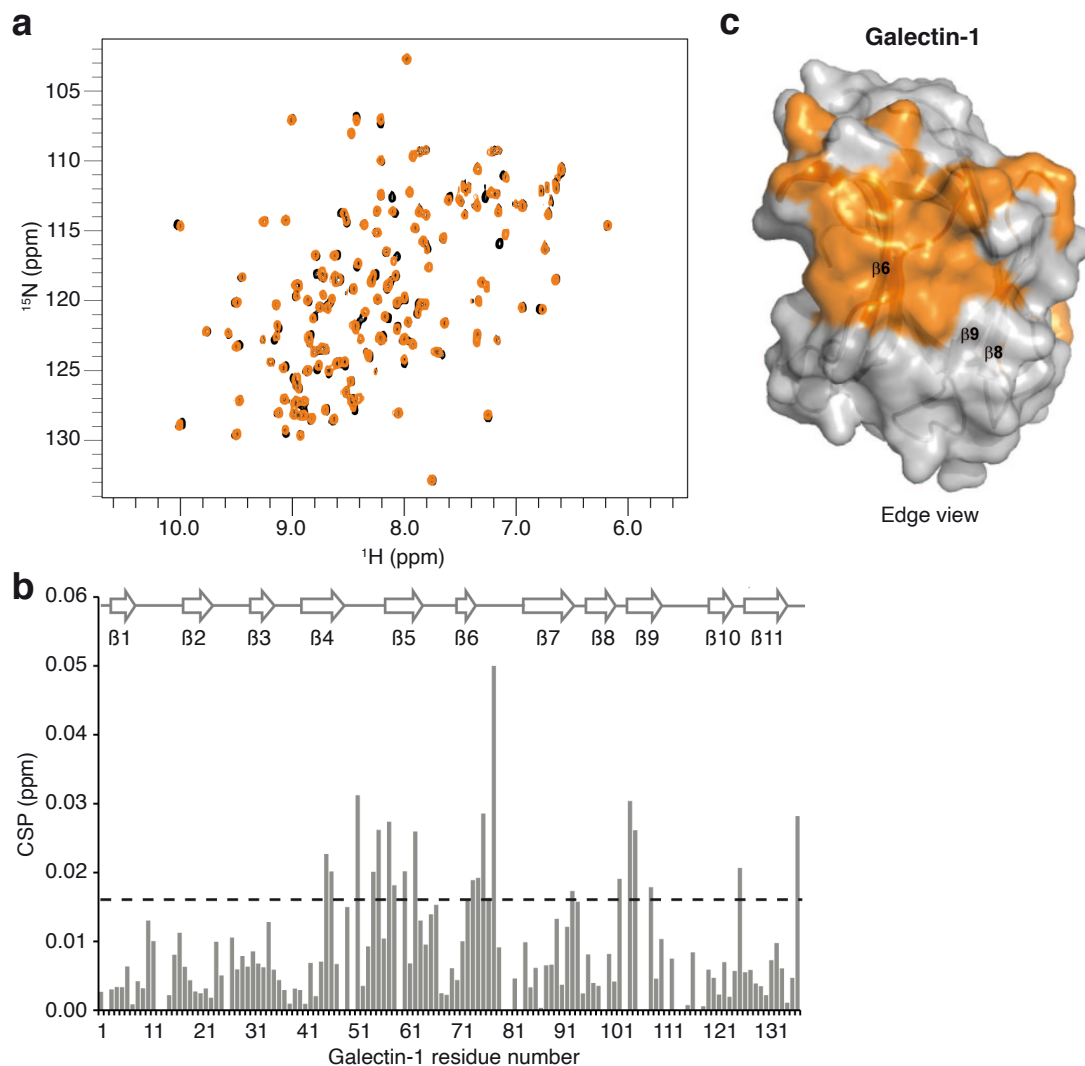
**Supplementary figure 2. Peak intensity ratio analysis of  $^{15}\text{N}$  amide probes of galectin-1.**



Normalized peak intensity ratio analysis ( $I/I_0$ ) of galectin-1 bound to CXCL4. Dotted lines represent  $1\sigma$  from the average  $I/I_0$ . Ratios below the threshold are colored in light orange.



**Supplementary Figure 3. Galectin-1 interaction to the CXCL4  $\beta$ -sheet region (CXCL4<sup>22-54</sup>).**

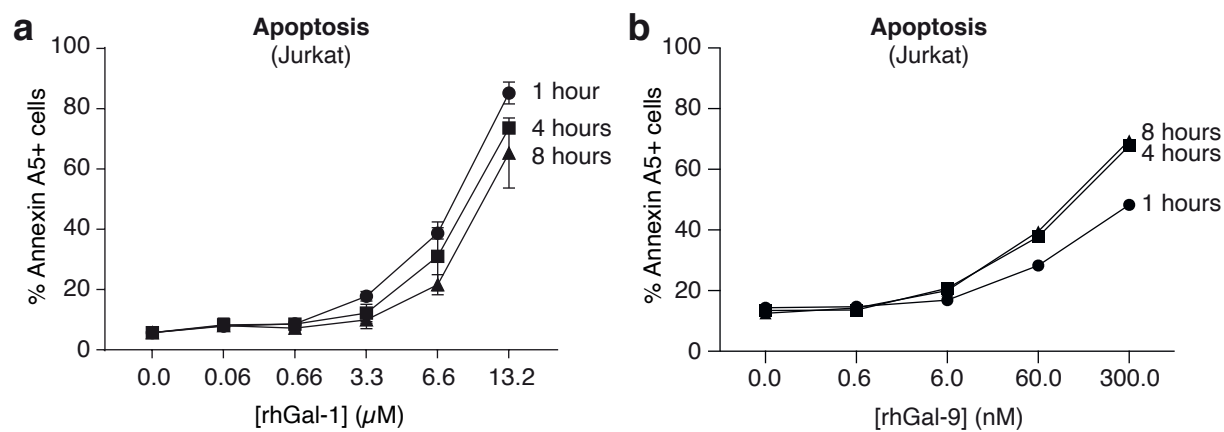


**a)** Overlay of  $^1\text{H}$ - $^{15}\text{N}$  HSQC spectra of  $^{15}\text{N}$ -labeled galectin-1 free (black trace) and bound to CXCL4<sup>22-54</sup> (orange trace).

**b)** Histogram plot of CSPs observed for each galectin-1 resonance upon interaction to CXCL4<sup>22-54</sup>. The dashed line represents  $1\sigma$  from the average CSP, thereby defining the threshold selection for the most affected residues. Galectin-1 secondary structures are depicted above the plot.

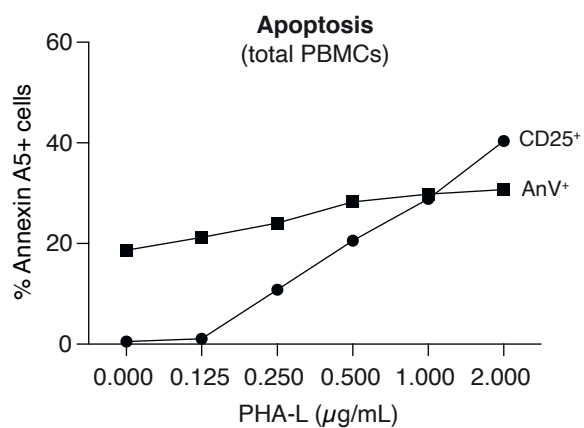
**c)** Chemical shift perturbation mapping onto galectin-1 monomer structure which is shown as a semitransparent solvent-accessible surface with a ribbon model displayed below the surface. Residues presenting CSPs above the threshold (defined in **(b)**) are colored in orange. Main  $\beta$ -strands affected are labeled.

**Supplementary Figure 4. Time- and concentration-dependent induction of Jurkat apoptosis by galectins.**



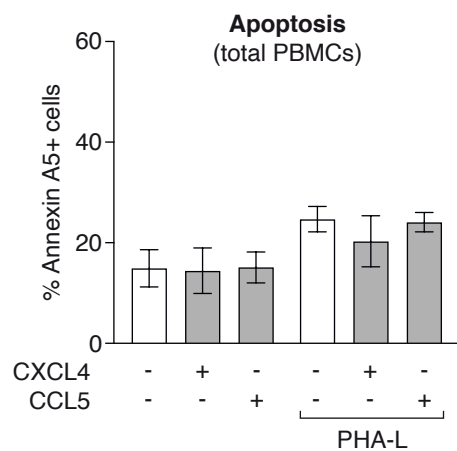
Jurkat cells were incubated during the indicated times and doses with galectin-1 (a) or galectin-9 (b). Apoptosis was assessed by annexin A5 and PI staining and FACS analysis. Graphs show data from at least 3 independent experiments.

**Supplementary Figure 5. Analysis of concentration-dependent immune cell activation by PHA-L treatment.**



PBMCs were treated for 24 hours with phytohemagglutinin-L (PHA-L) at the indicated concentrations. Apoptosis was assessed by FACS using annexin A5. Cell activation was assessed by FACS using CD25 staining.

# Supplementary Figure 6. Chemokines do not affect apoptosis of resting and activated PBMCs



Apoptosis as determined by FACS analysis (Annexin A5<sup>+</sup> and PI<sup>+</sup> staining). Both resting and activated peripheral blood mononuclear cells (PBMCs) were incubated for 24 hours with 12  $\mu$ M CXCL4 or 36 nM CCL5. PBMC-activation was induced by 24 hours treatment with 1  $\mu$ g/mL phytohemagglutinin-L (PHA-L) prior to treatment with chemokines. n = 2/3

Figures

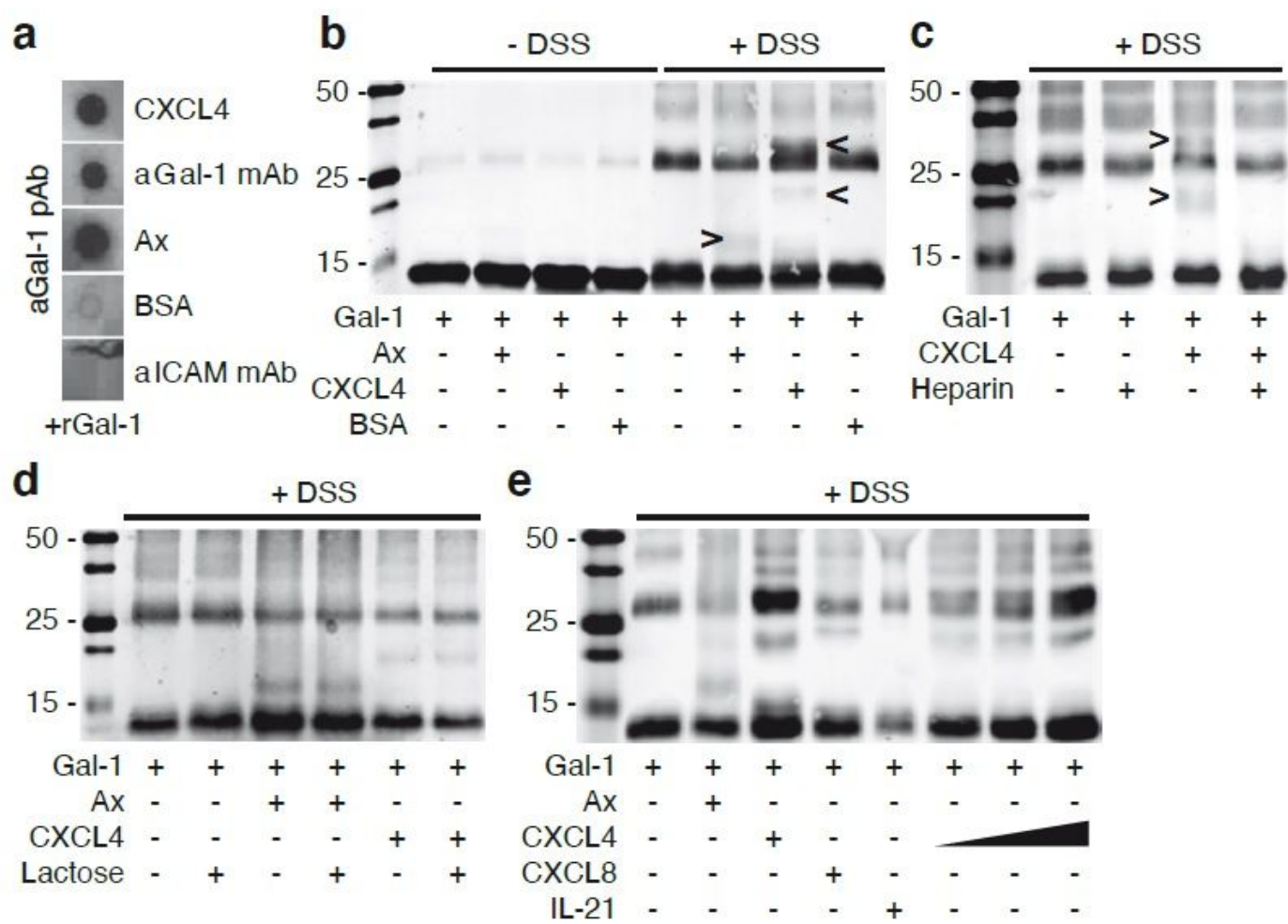
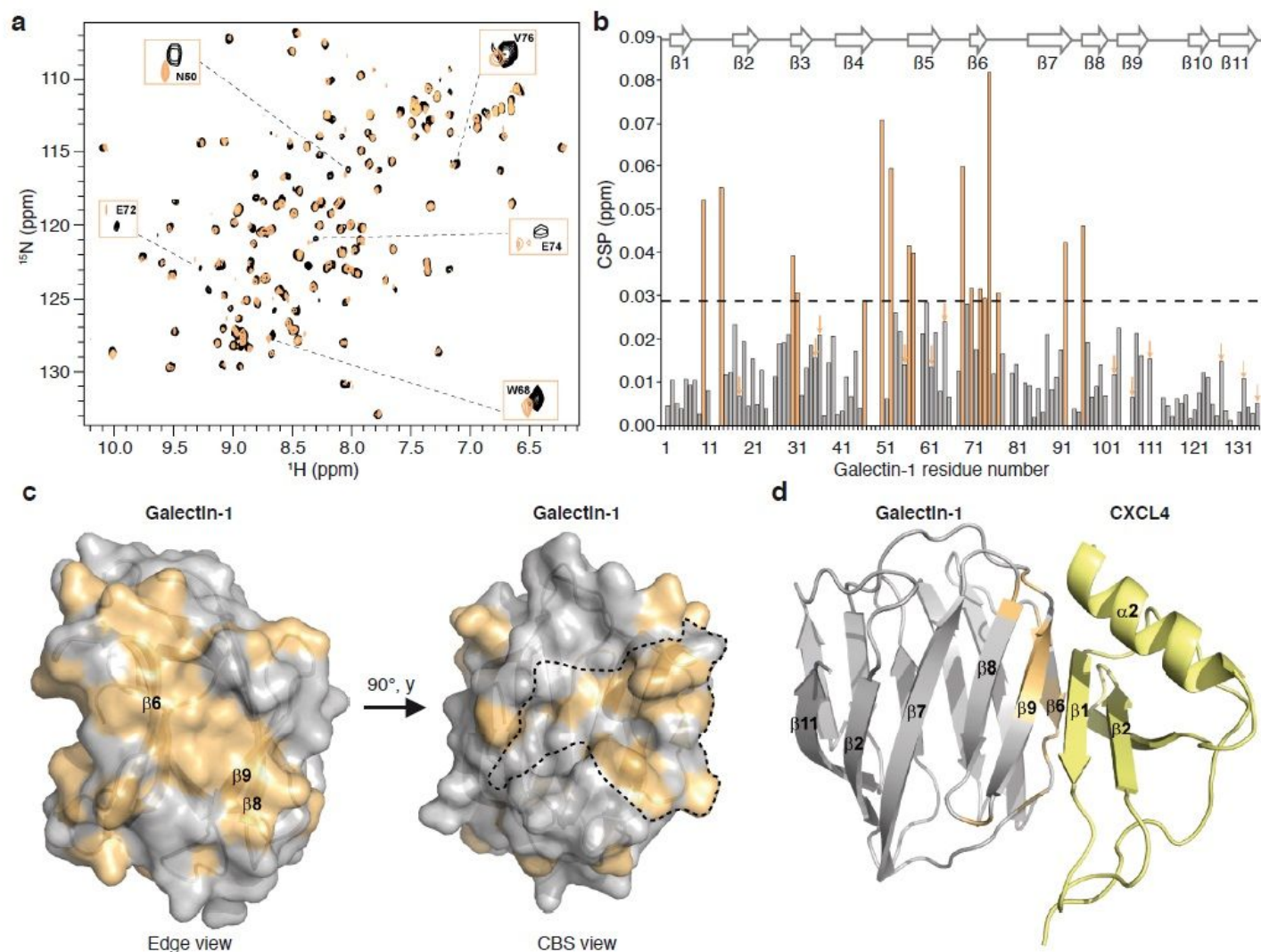


Figure 1

a) Representative spot blot analysis. Indicated proteins were spotted onto nitrocellulose filter and following incubation with galectin-1 protein-protein interaction was revealed by staining with anti-galectin-1 antibody. Anginex (Ax) and anti-galectin-1 monoclonal antibody served as positive controls, bovine serum albumin (BSA) and anti-ICAM monoclonal antibody served as negative control. b) Representative gel-shift analysis. Proteins (0.2 mg/mL) were incubated for 2 hours in the presence or absence of cross-linking agent disuccinimidyl suberate (DSS). Standard Western blot with anti-galectin-1 polyclonal antibody. The arrowheads point towards a shift of galectin-1. c) Similar as in (b) but in the presence or absence of excess heparin. d) Similar as in (b) but in the presence or absence of excess  $\beta$ -lactose. e) Similar as in (b) but in the presence of different cytokines or increasing concentrations of CXCL4.



**Figure 2**

a) Overlay of  $^1\text{H}$ - $^{15}\text{N}$  HSQC spectra of  $^{15}\text{N}$ -labeled galectin-1 free (black trace) and bound to CXCL4 (light orange trace). b) Histogram plot of CSPs observed for each galectin-1 resonance upon interaction to CXCL4. The dashed line represents 1s from the average CSP, thereby defining the threshold selection for the most affected residues. Light orange bars correspond to CSP above the threshold. Arrows are pointing toward residue showing significant intensity decrease upon interaction to CXCL4 (Supplementary figure 2). Galectin-1 secondary structures are depicted above the plot. c) Chemical shift perturbation mapping onto galectin-1 monomer structure which is shown as a semitransparent solvent-accessible surface with a ribbon model displayed below the surface. Residues presenting CSPs above the threshold (defined in (b)) are colored in light orange. Main  $\beta$ strands affected are labeled. Two galectin-1 orientations are presented: (i) the galectin-1 edge view, opposite to the dimer interface, and (ii) the CBS view with the CBS boundaries plotted in dotted lines. a b c  $^{15}\text{N}$  (ppm)  $^1\text{H}$  (ppm) 110 130 115 125 120 10.0 9.5 9.0 8.5 8.0 7.5 7.0 6.5 0.09 CSP (ppm) 0.08 0.07 0.06 0.03 0.02 0.01 0.00 0.04 0.05 1 11 21 31 41 51 61 71 81 91 101 111 121 131 Galectin-1 residue number  $\beta 1$   $\beta 2$   $\beta 3$   $\beta 4$   $\beta 5$   $\beta 6$   $\beta 7$   $\beta 8$   $\beta 9$   $\beta 10$   $\beta 11$  d Edge view CBS view Galectin-1 Galectin-1 Galectin-1 CXCL4  $90^\circ$ , y d) The structural model of the galectin-

1/CXCL4 complex. Galectin-1 is shown as grey ribbon whereas CXCL4 is colored yellow. Galectin-1 residues found at the interface of the complex and presenting CSPs above the threshold (defined in (b)) are colored in light orange.

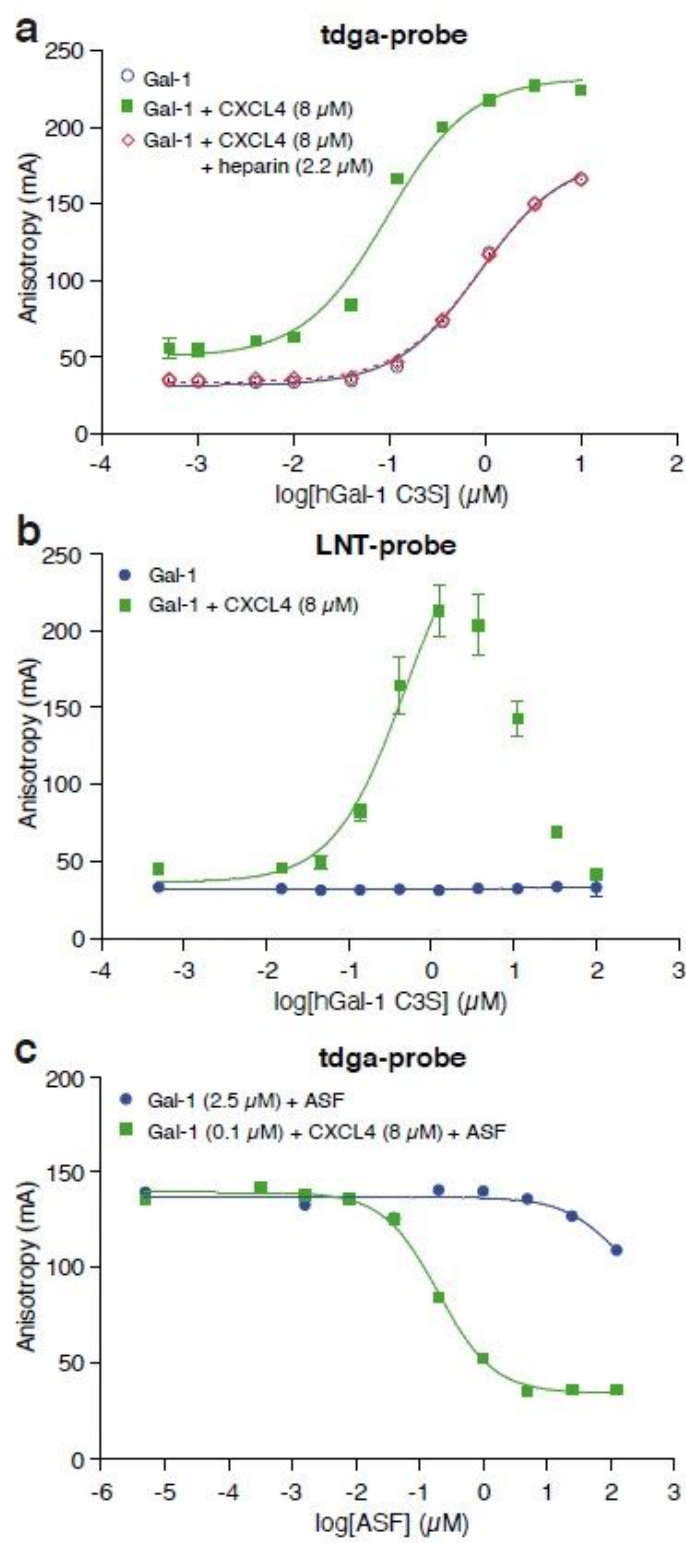


**Figure 3**

a) Anisotropy analyses using a fluorescently labeled high affinity thiodigalactoside amide (tdga)-probe with increasing galectin-1 concentrations in the absence (blue line, open circles) or presence (green line,



closed squares) of CXCL4 and excess heparin (red line, open diamonds). b) Anisotropy analyses using a fluorescently labeled low affinity lacto-N-triose (LNT)-probe with increasing galectin-1 concentrations in the absence (blue line, closed circles) or presence (green line, closed squares) of CXCL4. c) Anisotropy analyses using a fluorescently labeled high affinity tdga-probe with fixed galectin-1 concentrations and increasing concentrations of an unlabeled high affinity asialofetuin (ASF)-probe in the presence (green line, closed squares) and absence (blue line, closed circles) of CXCL4.

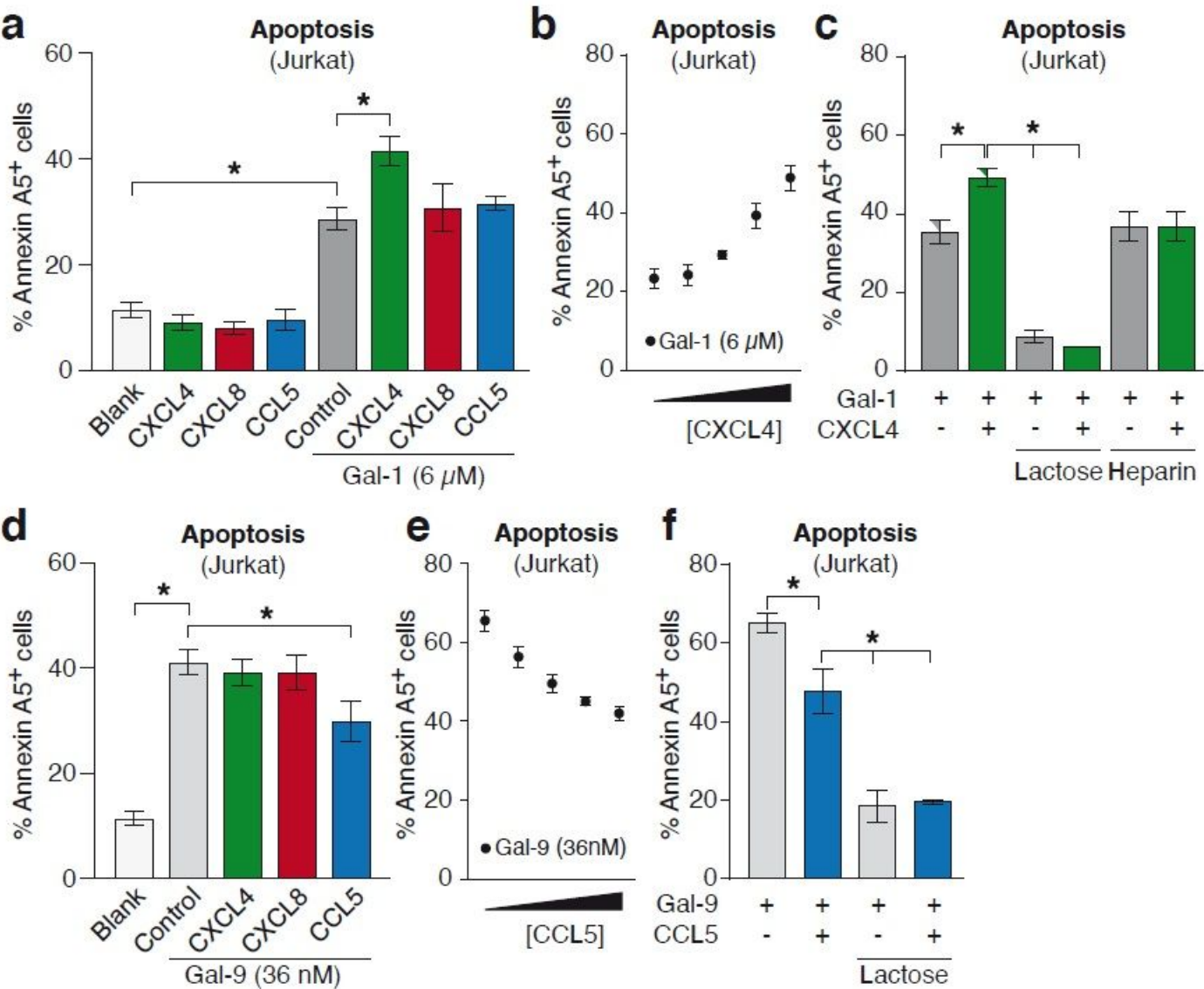


**Figure 4**

a) Apoptosis as determined by FACS analysis (Annexin A5<sup>+</sup> and PI<sup>+</sup> staining). Jurkat cells were incubated for 1 hour with 6 μM galectin-1 in the presence or absence of the indicated chemokines at equimolar concentrations. b) Similar as in (a) but with increasing concentrations of CXCL4 (0, 1.5, 3, 6 and 12 μM). c) Similar as in (a) but with the addition of either excess β-lactose or heparin d) Apoptosis as determined by FACS analysis (Annexin A5<sup>+</sup> and PI<sup>+</sup> staining). Jurkat cells were incubated for 4 hours with 36 nM galectin-9 in the presence or absence of the indicated chemokines at equimolar



concentrations. e) Similar as in (d) but with increasing concentrations of CCL5 (0, 9, 18, 36, 72 nM). f) Similar as in (d) but with the addition of excess lactose. Graphs show data from at least 5 independent experiments. \*p-value <0.05

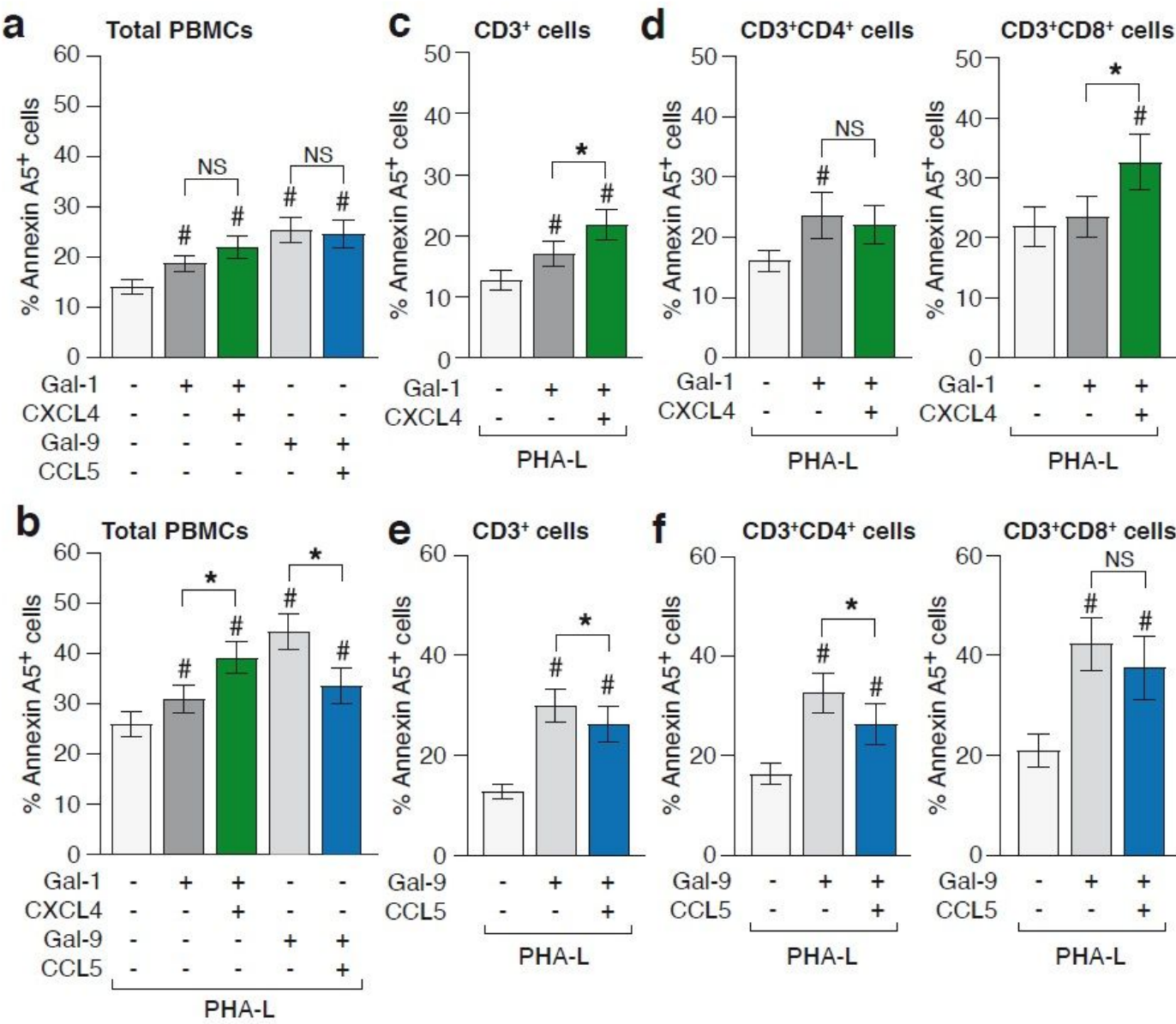


**Figure 5**

a) Apoptosis as determined by FACS analysis (Annexin A5<sup>+</sup>). Peripheral blood mononuclear cells (PBMCs) were incubated for 24 hours with 12 μM galectin-1 or 36 nM galectin-9 in the presence or absence of the indicated chemokines at equimolar concentrations. b) Similar as in (a) but PBMCs were activated for 24 hours with 1 μg/mL phytohemagglutinin-L (PHA-L) prior to treatment with galectins and chemokines. c-f) Treatment similar as in (b) followed by FACS analysis with gating for specific subpopulations, i.e. CD3<sup>+</sup>, CD3<sup>+</sup>/CD4<sup>+</sup>, CD3<sup>+</sup>/CD8<sup>+</sup>. Graphs show percentage of Annexin A5<sup>+</sup> cells within the indicated populations. At least six independent experiments were performed on PBMCs from different donors. # p-value <0.05 vs. untreated cells. \* p-value < 0.05.